JARQ 56 (3), 295-301 (2022) https://www.jircas.go.jp

Transcriptional Responses of the Marine Planktonic Diatom *Chaetoceros tenuissimus* to Nitrogen- and Phosphorus-deficient States

Haruo YAMAGUCHI[1]*, Minoru INOUE[1], Yuko TANIMOTO[1], Narumi SUMIDA[1], Masao ADACHI[1], Kei KIMURA[2] and Yuji TOMARU[3]

[1] Laboratory of Aquatic Environmental Science, Faculty of Agriculture and Marine Science, Kochi University, Nankoku, Japan
[2] Faculty of Agriculture, Saga University, Saga, Japan
[3] Fisheries Technology Institute, Japan Fisheries Research and Education Agency, Hatsukaichi, Japan

Abstract

Dissolved nutrients, especially inorganic nitrogen (N) and inorganic phosphorus (P), are typically deficient in the coastal surface waters of temperate regions during warm seasons. Even under the conditions of inorganic N and P deficiencies, the planktonic diatom *Chaetoceros tenuissimus* sometimes forms blooms. The present study characterized, at the mRNA transcript level, the gene expression patterns in N- or P-limited cultures of *C. tenuissimus* to propose the molecular markers of N- and P-deficient states of *C. tenuissimus*. Gene transcriptions of nitrate transporter and glutamine synthetase appeared to be upregulated in N-limited cultures. Phosphate transporter and alkaline phosphatase transcriptions appeared to be induced under P-limited conditions. These results suggest that *C. tenuissimus* under the N-deficient state expresses a transmembrane nitrate transporter, uptakes nitrate effectively, and assimilates the N source rapidly via glutamine synthesis; P-deficient *C. tenuissimus* possibly supplements P sources from organic P compounds via hydrolysis actions of phosphatases and uptakes phosphate effectively through phosphate transporters.

Discipline: Fisheries
Additional key words: phytoplankton, microarray

Introduction

Diatoms are unicellular eukaryotic algae found throughout the world's oceans, which account for a large part of marine primary production; up to 35% in oligotrophic oceans and 75% in nutrient-rich systems (Nelson et al. 1995). The genus *Chaetoceros* is highly diverse, with > 400 species that are considered to play important roles in primary production (Rines & Hargraves 1988). A small marine diatom, *Chaetoceros tenuissimus* Meunier, is widely distributed throughout the coastal waters of the Mediterranean Sea (Kooistra et al. 2010, Montresor et al. 2013), Black Sea (Baytut et al. 2013), Narragansett Bay (Rines & Hargraves 1988), and Japan (Toyoda et al. 2010, Tomaru et al. 2011, 2018). In Hiroshima Bay, Japan, *C. tenuissimus* often forms blooms during warm seasons (Toyoda et al. 2010, Tomaru et al. 2011). Two strains (NIES-3714 and NIES-3715) of this diatom can grow rapidly at 20°C-30°C (Tomaru et al. 2014), which suggests that warm waters seem to be preferable for the formation of *C. tenuissimus* blooms. Therefore, to understand coastal primary production, the growth and physiological characteristics of *C. tenuissimus* in warm coastal waters should be clarified.

Levels of nitrogen (N) and/or phosphorus (P) in warm coastal waters often limit the growth of phytoplankton and usually regulate primary production. Dissolved inorganic N and P in the euphotic zone are utilized by eukaryotic algae. Nevertheless, their concentration is often deficient, especially when the water bodies are stratified during warm seasons (Yamaguchi & Sai 2015). Such environments likely cause N stress and/or P stress of the coastal algae,

*Corresponding author: yharuo@kochi-u.ac.jp
Received 12 May 2021; accepted 7 October 2021.

including *C. tenuissimus*. Thus, the physiological responses of *C. tenuissimus* to N stress and/or P stress should play an important role in bloom dynamics and primary production in coastal waters. For elucidating the cell physiological states of *C. tenuissimus*, N-stress and P-stress markers will be useful to better understand the bloom dynamics.

This study comparatively examined the transcriptions of mRNA in *C. tenuissimus* cultures under nutrient-replete, N-limited, and P-limited conditions. The candidate genes, which appear to be induced strongly in the nutrient-limited states of *C. tenuissimus*, were obtained through microarray analyses. The mRNA transcriptions of the significant genes associated with the utilization of N and P were quantified using quantitative reverse transcription–polymerase chain reaction (qRT-PCR). Based on the results, we propose significant and useful molecular markers for understanding the physiological states of *C. tenuissimus*.

Materials and methods

1. Cultures and samples

A clonal axenic strain (NIES-3715, formerly 2-10) of *Chaetoceros tenuissimus* was used. These stock cultures were maintained in a modified SWM-3 medium (Chen et al. 1969), at 20°C, under a 12:12 h light/dark photocycle at 186 µmol photons m^{-2} s^{-1} (light source: cool-white fluorescent tubes). According to Imai et al. (1996), Na_2SeO_3 was added at a final concentration of 2 nM into the SWM-3 media. The cell suspensions were inoculated into three kinds of SWM-3 media contained in Erlenmeyer flasks: nutrient-replete (+NP), 2 mM NO_3, and 65 µM PO_4; N-depleted (−N), 75 µM NO_3, and 65 µM PO_4; and P-depleted (−P), 2 mM NO_3, and 1 µM PO_4. Cultures were incubated at duplicate under the same conditions as the preincubation period. By measuring the time-course of *in vivo* chlorophyll *a* fluorescence (relative fluorescence unit) using a Turner Fluorometer (Sunnyvale), we estimated the growth of the cultures. Cultures of *C. tenuissimus* were deemed to be −N and −P states when their chlorophyll *a* fluorescences were lower than that in the +NP culture.

Cell suspensions were transferred into 250 mL centrifuge bottles (3140, NALGEN), and the bottles were centrifuged at 20°C, 3,000 rpm × 10 min. The harvested cell pellets were transported into 1.5 mL microtubes and stored at −70°C before RNA extraction. Using RNeasy Plant Mini Kit (Qiagen®) and RNase-free DNaseSet (Qiagen®), RNA in cells was extracted and purified. These procedures were conducted according to the company manuals. Genomic DNA of *C. tenuissimus* 2-10 cultivated with +NP media was extracted using a DNeasy kit (Qiagen®), according to the manufacturer's instructions.

2. Microarray analysis

Partial genome sequences and microarray analyses were conducted in contract services of Roche. Partial genome sequences were analyzed using the GS FLX system (Roche Ltd.), according to the manufacturer's instructions. The sequence data were automatically assembled using GS De Novo Assembler v2.3 (Newbler) (Roche Ltd). Putative open reading frames (ORFs) of 12,710 found in phytoplankton genomes were targeted in the design of microarray probes. Microarray analyses were conducted using probes that were automatically designed with a program of NimbleGen. For one putative ORF, five probes were designed.

The cDNA was synthesized from the RNA sample with a SuperScript Double-Stranded cDNA Synthesis Kit (Invitrogen) and then labeled using a NimbleGen One-Color DNA Labeling Kit. The Cy3-labeled cDNA was hybridized to a NimbleGen gene expression microarray at 42°C for 16 h-20 h. The microarray was washed using a NimbleGen Wash Buffer Kit and then scanned with a NimbleGen MS200 Microarray Scanner. The signal fluorescence intensity from each probe was measured as an indicator of RNA transcription with a NimbleScan v2.5. RNA transcription was compared among +NP, −N, and −P treatments by using the scatter plots obtained with a NANDEMO Analysis 1.0.2 software (Roche). To select the significant genes associated with N and P utilization by *C. tenuissimus*, significantly upregulated and downregulated ($P < 0.05$, ≥ 10 fold) genes in −N and −P treatments were determined by statistically comparing with +NP treatment (*t*-test, $\alpha = 0.05$). Significantly regulated genes were determined using BLASTX searching.

3. Quantitative reverse transcription–polymerase chain reaction

Putative nitrate transporter (NRT, LC317057), glutamine synthetase (GS, LC317058), alkaline phosphatase (PhoA, LC317056), and phosphate transporter (P_iT, LC317055) genes were tested. cDNA was synthesized from the RNA sample with a SuperScript First Strand Synthesis System for RT-PCR (Invitrogen), according to the manufacturer's instructions. RNA concentrations of samples were measured before cDNA synthesis with a spectrophotometer (DU-730, BECKMAN COULTER) and then adjusted to a constant concentration by diluting

the samples. The PCR mixture was prepared according to the manufacturer's instructions; Power SYBR® Green PCR Master Mix (Thermo Fisher Scientific) 12.5 µL, 20 µM forward and reverse primers 0.25 µL (Table 1), cDNA sample 1.0 µL, and RNase-free water 11.25 µL were mixed in a tube of 0.2 mL 8-Strip PCR tube (Greiner Bio-One). The real-time PCR cycles comprised 10 min at 95°C, followed by 40 cycles of 95°C for 15 s and 60°C for 60 s. The obtained threshold cycle value (C_T) was used to determine the target gene's expression. Expression values of the target genes were relatively determined by using the comparative C_T method ($\Delta\Delta C_T$ method), wherein 28S rRNA, 18S rRNA, and actin were used as reference genes. Finally, relative expression values were determined as $2^{-\Delta\Delta C_T}$. Differences between the average abundances obtained for each treatment were analyzed using Tukey's multiple comparison test ($\alpha = 0.05$).

Results and discussion

In −N and −P cultures of *C. tenuissimus*, *in vivo* chlorophyll *a* fluorescence yields (relative unit) were 77.5 and 53.5 (Fig. 1). These values were lower than 88.5 (exponential phase) and 156 (stationary phase) of control (+NP media, Fig. 1). Then, many transcripts were obtained from the −N, −P, and +NP cultures of *C. tenuissiumus*. Compared with transcripts in NP-replete, the selected transcripts that were significantly upregulated and downregulated ($P < 0.05$ and ≥ 10 fold)

Table 1. Primers used for real-time PCR

Target putative gene	Forward (5′-3′)	Reverse (5′-3′)
Nitrate transporter	TTGTTGGAGCTGGAGGAAACTC	TGGCAACTGACGGAAGCA
Glutamine synthetase	TGCCAGAGCTCCGTAAGGTT	TCCACAACTCAGCAGGAACAAC
Phosphate transporter	TCGGTGGTGAAGTAGGCTACAA	TCCATCCTCTTCGAAACATCCT
Phosphomonoesterase	GCGAAGGCTGCATTTGCT	CCGTGTCCTTGTCCCTCAGT
Actin-like	AGAGGCGCACCCAGTTCTC	CGCTCACGGTTTGCCTTT
18S rRNA	TTTAATCCTCTTGCCTCGTCCTT	TGAGCGGCTATCTCCTCGAT
28S rRNA	ATCTCTTGGAACAGGGTGCCTAT	AAAGCCAAGGCCAGAAGCTAT

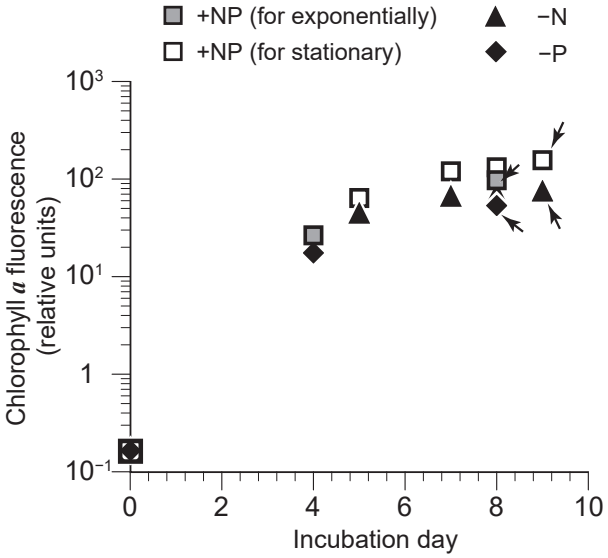

Fig. 1. Growth of *Chaetoceros tenuissimus* cultures under the conditions of nutrient-replete (+NP), nitrogen deficiency (−N), and phosphorus deficiency (−P)
+NP cultures are used for sampling cell suspension in exponentially and stationary phases.
Arrows indicate sampling time.

are shown, together with specific gene sequences (Tables 2, 3).

A considerable number of genes identified as NRT and glutamine synthethase (GS, 04999_orf00005) and others appeared to be strongly upregulated in −N cultures compared with in +NP cultures. The genes of alkaline phosphatase (PhoA) were strongly induced in −P cultures; phosphate transporter (P_iT), phosphoenolpyruvate synthase, and NADPH nitrite reductase also appeared to be upregulated (Tables 2, 3). Contrary to −N treatment, GS (28390_orf00003), whose sequences appeared to be different from those of GS (04999_orf00005), were downregulated.

The cycle threshold values of actin, 18S rRNA, and 28S rRNA in *C. tenuissimus* cultures were 21.8 ± 0.83, 18.4 ± 0.49, and 16.4 ± 0.19, respectively. As supported by a low coefficient of variation, this gene expression did not vary dramatically among the +NP exponential, +NP stationary, −P stationary, and −N stationary phases. When the internal references were used, mRNA transcripts of NRT and GS appeared in cultures of the stationary phase and were induced significantly ($P < 0.05$) in a N-deficient state (Fig. 2). Expressions of phosphate transporter and alkaline phosphatase were

Table 2. Microarray results—properties of sequences found in nitrogen-deficient cultures of *Chaetoceros tenuissimus* with their relative expression (fold changes) to those in nutrient-replete cultures of this diatom

Contig No.	Fold changes	UP/DOWN	*P* value	E value[a]	Matched gene
16813_orf00002	64.7	UP	5.28×10^{-7}	8×10^{-11}	Drug/Metabolite transporter (DMT) Superfamily putative (*Albugo laibachii* Nc14)
03171_orf00005	51.4	UP	1.43×10^{-8}	6×10^{-91}	Sodium symporter family [*Micromonas* sp. RCC299]
			1.43×10^{-8}	6×10^{-6}	High affinity choline transporter [*Cellvibrio japonicus* Ueda107]
03171_orf00007	29.2	UP	1.77×10^{-7}	7×10^{-69}	Sodium symporter family [*Micromonas* sp. RCC299]
				8×10^{-28}	Na^+/Proline symporter PutP [*Acaryochloris marina* MBIC11017]
				3×10^{-14}	High affinity choline transporter 1 [*Cupriavidus necator* N01]
29751_orf00001	30.3	UP	2.00×10^{-5}	8×10^{-14}	Xanthine/Uracil permiase [*Phaeodactylum tricornutum* CCAP1055/1]
29751_orf00002	47.5	UP	1.08×10^{-7}	5×10^{-11}	Xanthine/Uracil permiase [*Phaeodactylum tricornutum* CCAP1055/1]
				6×10^{-7}	Purine transporter [*Pyrenophora tritici-repentis* Pt-1C-BFP]
03899_orf00004	26.3	UP	6.74×10^{-6}	6×10^{-9}	Predicted: similar to putative ascorbate peroxidase [*Hydra magnicapilata*]
35032_orf00004	18.5	UP	2.13×10^{-5}	3×10^{-4}	Hydrolase, alpha/beta fold family [*Moritella* sp. PE36]
36881_orf00004	18.0	UP	2.51×10^{-5}	8×10^{-4}	HI-5α: Heat-shock protein [*Chaetoceros compressum*]
27400_orf00003	15.8	UP	7.46×10^{-6}	3×10^{-23}	Ubiquinol:cytochrome c oxidoreductase biogenesis factor [*Chlamydomonas reinhardtii*]
				1×10^{-22}	bcs1 aaa-type ATPase, putative [*Ectocarpus ailiculosus*]
00295_orf00004	15.8	UP	6.00×10^{-6}	6×10^{-13}	Trichohyalin, putative [*Ricinus communis*]
				9×10^{-13}	KRR1 family protein [*Arabidopsis thaliana*]
17113_orf00002	15.4	DOWN	2.23×10^{-6}	2×10^{-9}	Oxidoreductase [*Phaeodactylum tricornutum* CCAP1055/1]
					2-Hydroxy-3-oxopropinate reductase [*Geobacter* sp. M18]
37203_orf00003	15.3	UP	3.74×10^{-5}	$< 10^{-100}$	Putative nitrate transporter [*Skeletonema costatum*]
				$< 10^{-100}$	Nitrate transporter [*Thalassospira pseudonana* CCMP1335]
00295_orf00003	15.1	UP	1.55×10^{-6}	4×10^{-5}	Predicted: similar to slenderb lobes, putative [*Nasonia vitripennis*]
				2×10^{-5}	Ribosome biogenesi protein Kri1 [*Aspergillus oryzae* RIB40]
14483_orf00001	15.0	UP	3.32×10^{-6}	8×10^{-16}	Fructose-6-phosphate phophoketolase [*Chlorobium ferrooxidans* DSM 13031]
00816_orf00001	14.4	UP	5.66×10^{-6}	2×10^{-14}	Putative nitrate transporter [*Thalassiospira weissflogii*]
				1×10^{-13}	Nitrate transporter [*Thalassospira pseudonana* CCMP1335]
04999_orf00005	13.8	UP	5.71×10^{-4}	$< 10^{-100}$	Glutamine synthetase type III [*Chaetoceros compressus*]
				$< 10^{-100}$	GLNA, glutamine synthetase [*Phaeodactylum tricornutum* CCAP1055/1]
34639_orf00003	13.3	UP	4.22×10^{-6}	1×10^{-43}	NADH-dependent fumarate reductase-like protein [*Leishmania mexicana* MHOM/GT/2001/U1103]
				7×10^{-28}	NADH-cytochrome b5 reductase [*Dictyostelium discoideum* AX4]
				2×10^{-27}	Nitrate reductase 2 [*Puccinia graminis* f. sp. *tritici* CRL 75-36-700-3]
29605_orf00001	12.7	UP	9.23×10^{-8}	1×10^{-13}	Cell surface protein [*Epulopiscium* sp. 'N.t. morphotype B']
00295_orf00001	12.6	UP	3.09×10^{-6}	2×10^{-5}	Eukaryotic translation initiation factor 5B, putative [*Perkinsus marinus* ATCC50983]
				2×10^{-5}	Glutamine-asparagine rich protein, putative [*Perkinsus marinus* ATCC 50983]
29165_orf00001	12.5	UP	2.33×10^{-2}	1×10^{-46}	Demethylmenaquinone methyltransferase/aldolase [*Micromonas* sp. RCC299]
				1×10^{-44}	Putative 4-hydroxyphenyllacetate isomerase/decar (ISS) [*Ostreococcus tauri*]
54575_orf00007	12.3		4.58×10^{-4}	1×10^{-65}	NADH-dependent fumarate reductase, putative [*Trypanosoma cruzi*]
				1×10^{-61}	Mitochondrial NADH-dependent fumarate reductase [*Trypanosoma brucei*]
20980_orf00001	11.2	DOWN	8.82×10^{-8}	5×10^{-13}	Transketolase [*Phaeodactylum tricornutum* CCAP 1055/1]

[a]The expect value in BLAST search means the number of expected hits of similar quality that could be found just by chance.
Gray-shaded areas mean the gene sequences; these expressions were also quantified by PCR-based methods as shown in Figure 2.

Table 3. Microarray results—properties of sequences found in phosphorus-deficient cultures of *Chaetoceros tenuissimus* with their relative expression (fold changes) to those in nutrient-replete cultures of this diatom

Contig No.	Fold changes	UP/DOWN	*P* value	E value[a]	Matched gene
29884_orf00001	93.8	UP	4.81×10^{-5}	2×10^{-3}	Predicted protein [*Phaeodactylum tricornutum* CCAP1055/1]
				2.4	Alkaline phosphatase, putative [*Cyanobium* sp. PCC 7001]
05580_orf00001	28.73	DOWN	3.00×10^{-4}	$< 10^{-99}$	RL3, Ribosomal protein 3, 60S large ribosormal subunit [*Thalassiosira pseudonana* CCMP1335]
20842_orf00002	28.46	DOWN	4.10×10^{-6}	5×10^{-11}	Enoyl-reductase [NADH] [*Thalassiosira pseudonana* CCMP1335]
16748_orf00001	24.19	DOWN	6.90×10^{-6}	1×10^{-31}	RS5, Ribosomal protein 5 [*Thalassiosira pseudonana* CCMP1335]
04076_orf00001	23.92	DOWN	1.10×10^{-4}	2×10^{-58}	RL4e, Ribosomal protein 4e 60S large subunit [*Thalassiosira pseudonana* CCMP1335]
05387_orf00002	21.93	UP	2.23×10^{-5}	9×10^{-54}	Phophoenolpyruvatre synthase [*Cyanothece* sp. PCC7424]
28807_orf00001	21.25	DOWN	3.57×10^{-6}	8×10^{-60}	RL5, Ribosomal protein 5, 60S large ribosomal subunit [*Thalassiosira pseudonana* CCMP 1335]
34152_orf00001	21.14	DOWN	5.75×10^{-5}	2×10^{-57}	40S Ribosomal protein S3-3 NADPH nitrite reducatase [*Thalassiosira pseudonana* CCMP 1335]
27667_orf00005	20.70	DOWN	8.47×10^{-4}	$< 10^{-100}$	40S Ribosomal protein-like protein [*Thalassiosira pseudonana* CCMP 1335]
28807_orf00003	19.90	DOWN	1.43×10^{-3}	8×10^{-46}	RL5, Ribosomal protein 5, 60S large ribosomal subunit [*Thalassiosira pseudonana* CCMP 1335]
05328_orf00002	18.70	UP	5.28×10^{-3}	2×10^{-95}	NADPH nitrite reducatase [*Thalassiosira pseudonana* CCMP 1335]
16620_orf00002	18.21	DOWN	1.35×10^{-4}	5×10^{-81}	ATP sulfurylase (sulfate adenylyltransferase) [*Ostreococcus lucimarinus* CCE9901]
03104_orf00003	17.87	UP	2.12×10^{-4}	$< 10^{-100}$	Sodium phosphate cotransporter, Na/Pi cotransport system protein [*Thalassospira pseudonana* CCMP1335]
16290_orf00001	17.83	DOWN	8.07×10^{-5}	9×10^{-32}	RL9, Ribosomal protein 9 [*Thalassiosira pseudonana* CCMP 1335]
05328_orf00003	17.75	UP	9.81×10^{-6}	5×10^{-8}	NADPH nitrite reducatase [*Thalassiosira pseudonana* CCMP 1335]
04481_orf00007	17.65	DOWN	1.05×10^{-4}	7×10^{-75}	RS9, Ribosomal protein 9 [*Thalassiosira pseudonana* CCMP 1335]
34152_orf00003	17.58	DOWN	2.10×10^{-3}	5×10^{-23}	RL5, Ribosomal protein 5, 60S large ribosomal subunit [*Thalassiosira pseudonana* CCMP 1335]
11360_orf00003	17.01	DOWN	4.98×10^{-7}	$< 10^{-100}$	RL5, Ribosomal protein 5, 60S large ribosomal subunit [*Thalassiosira pseudonana* CCMP 1335]
20842_orf00001	17.00	DOWN	1.63×10^{-3}	2×10^{-23}	RL5, Ribosomal protein 5, 60S large ribosomal subunit [*Thalassiosira pseudonana* CCMP 1335]
03047_orf00002	16.72	DOWN	5.73×10^{-7}	$< 10^{-90}$	RL5, Ribosomal protein 5, 60S large ribosomal subunit [*Thalassiosira pseudonana* CCMP 1335]
06539_orf00003	16.58	DOWN	1.59×10^{-4}	2×10^{-32}	RL5, Ribosomal protein 5, 60S large ribosomal subunit [*Thalassiosira pseudonana* CCMP 1335]
27116_orf00001	16.55	DOWN	2.34×10^{-3}	9×10^{-98}	RL5, Ribosomal protein 5, 60S large ribosomal subunit [*Thalassiosira pseudonana* CCMP 1335]
27523_orf00013	16.32	DOWN	5.58×10^{-5}	1×10^{-91}	Adenine nucleotide translocator, ATP/ADP translocase [*Thalassiosira pseudonana* CCMP 1335]
08192_orf00004	16.12	DOWN	7.79×10^{-5}	6×10^{-52}	RL13e, Ribosomal protein 13e 60S large ribosomal subunit [*Thalassiosira pseudonana* CCMP1335]
01839_orf00001	16.02	DOWN	0.02	2×10^{-68}	Nucleoside diphosphate kinase 3 [*Phaeodactylum tricornutum* CCAP 1055/1]
11633_orf00002	16.00	DOWN	1.12×10^{-3}	$< 10^{-100}$	60S Acidic ribosomal protein P0 putative [*Albugo laibachii* Nc14]
28390_orf00003	15.57	DOWN	6.26×10^{-4}	$< 10^{-100}$	Gutamine synthetase [*Skeletonema costatum*]
					Glutamate ammonia ligase [*Ectocarpus siliculosus*]
05886_orf00002	15.46	UP	3.13×10^{-3}	2×10^{-17}	Glycerophosphoryl diester phosphodiesterase [*Clostridiales bacterium* 1_7_47_FAA]
29884_orf00004	15.39	UP	5.05×10^{-4}	2×10^{-30}	Alkaline phosphatase-like protein [*Thalassiosira pseudonana* CCMP1335]
					Glycerophosphoryl diester phosphodiesterase [*Cyanothece* sp. CCY0110]
13822_orf00004	14.40	DOWN	3.54×10^{-6}	3×10^{-67}	RL17, Ribosomal protein 17-like 60S large ribosomal subunit [*Thalassiosira pseudonana* CCMP1335]
36902_orf00002	14.27	DOWN	1.16×10^{-4}	3×10^{-15}	Hypothetical protein GCWU000323_01619 [*Leptotrichia hofstadii* F0254]
				1×10^{-14}	Methenyltetrahydrofolate cyclohydrolase [*Leptotrichia buccalis* DSM 1135]
05387_orf00003	14.11	UP	4.07×10^{-3}	0.13	Phosphoenolpyruvate synthase [*Nitrococcus mobilis* Nb-231]
05785_orf00001	13.82	DOWN	9.68×10^{-5}	4×10^{-56}	RL26, Ribosomal protein 26 60S large ribosomal subunit [*Thalassiosira pseudonana* CCMP1335]
06603_orf00001	13.17	DOWN	2.57×10^{-6}	1×10^{-96}	RL15, Ribosomal protein 15 60S large ribosomal subunit [*Thalassiosira pseudonana* CCMP1335]
32724_orf00001	12.90	DOWN	3.43×10^{-5}	2×10^{-6}	Putative ethylene-responsive RNA helicase (ISS) [*Ostreococcus tauri*]
18960_orf00001	12.80	DOWN	1.63×10^{-3}	2×10^{-66}	RL7, Ribosomal protein 7 [*Thalassiosira pseudonana* CCMP1335]
07516_orf00001	12.80	DOWN	1.43×10^{-4}	2×10^{-12}	Glutamate synthase [*Thalassiosira pseudonana* CCMP1335]
32968_orf00001	12.71	DOWN	0.02	4×10^{-35}	RS24, Ribosomal protein 24 40S small ribosomal subunit [*Thalassiosira pseudonana* CCMP1335]
08702_orf00005	12.68	UP	2.14×10^{-3}	3×10^{-7}	Predicted protein [*Thalassiosira pseudonana* CCMP1335]
05333_orf00007	12.61	DOWN	3.07×10^{-3}	2×10^{-4}	Predicted: mpv17-like protein-like isoform 2 [*Macaca mulatta*]
27592_orf00002	12.21	DOWN	1.28×10^{-4}	$< 10^{-100}$	Glutamate synthase [*Thalassiosira pseudonana* CCMP1335]
03765_orf00002	11.82	UP	2.38×10^{-4}	6×10^{-6}	SPX domain-containing protein [*Arabidopsis lyrata* subsp. *lyrata*]
				8×10^{-6}	Xenotropic and polytropic murine leukemia virus receptor ids-4, putative [*Ricinus communis*]
28505_orf00002	11.65	DOWN	7.67×10^{-6}	3×10^{-17}	Elongation factor Ts [*Idiomarina loihiensis* L2TR]
				3×10^{-16}	Translation elongation factor Ts [*Pectobacterium wasabiae* WPP163]
09479_orf00001	11.63	UP	3.70×10^{-3}	9×10^{-57}	Predicted protein [*Thalassiosira pseudonana* CCMP1335]
17261_orf00001	11.47	DOWN	8.85×10^{-3}	3×10^{-29}	40S Ribosomal protein S14 [*Danio rerio*]
05387_orf00006	11.43	UP	6.05×10^{-6}	$< 10^{-100}$	Phosphoenolpyruvate synthase [*Lyngbya* sp. PCC 8106]
04703_orf00001	11.22	DOWN	3.20×10^{-4}	$< 10^{-100}$	RL18, Ribosomal protein 18, 60S large ribosomal subunit [*Thalassiosira pseudonana* CCMP1335]
20987_orf00001	11.01	DOWN	6.50×10^{-6}	4×10^{-7}	RS25, Ribosomal protein 25 40S small ribosomal subunit [*Thalassiosira pseudonana* CCMP1335]
37427_orf00003	10.88	DOWN	9.62×10^{-3}	2×10^{-70}	60S Ribosomal protein L7a [*Zea mays*]
07469_orf00002	10.78	DOWN	1.86×10^{-5}	1×10^{-44}	RL6, Ribosomal protein 6 [*Thalassiosira pseudonana* CCMP1335]
05267_orf00001	10.53	DOWN	1.55×10^{-3}	$< 10^{-100}$	RL10, Ribosomal protein 10 60S large ribosomal subunit [*Thalassiosira pseudonana* CCMP1335]
14483_orf00001	10.34	UP	1.36×10^{-5}	7×10^{-16}	Phosphoketolase [*Pelodictyon phaeoclathratiforme* BU-1]
04010_orf00001	10.28	DOWN	4.99×10^{-4}	$< 10^{-100}$	Methionine S-adenosyl transferase [*Ditylum brightwellii*]

[a]The expect value in BLAST search means the number of expected hits of similar quality that could be found just by chance.
Gray-shaded areas mean the gene sequences; these expressions were also quantified by PCR-based methods as shown in Figure 2.

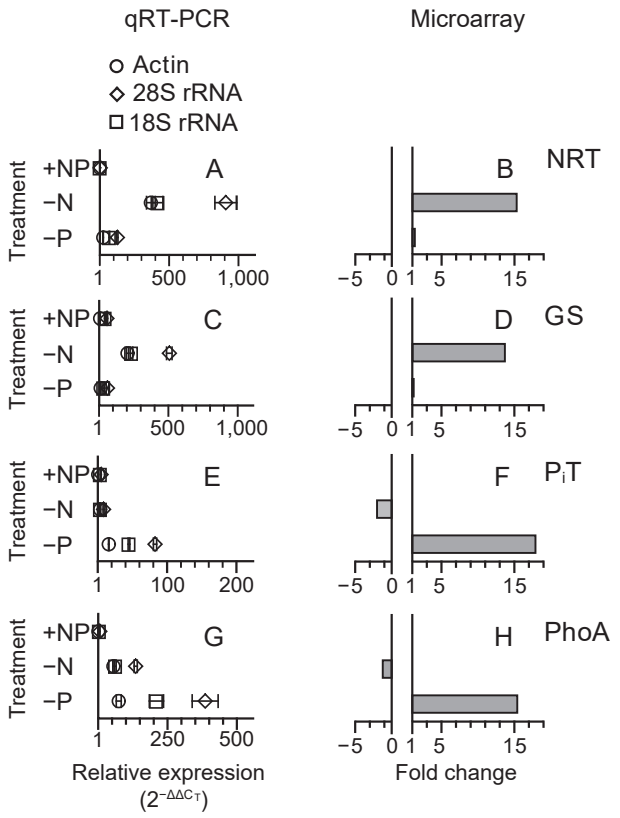

Fig. 2. Relative expression of the genes of nitrate transporter (NRT; A and B), glutamine synthetase (GS; C and D), phosphate transporter (PiT; E and F), and alkaline phosphatase (PhoA; G and H) in nutrient-replete (+NP), nitrogen-deficient (−N), and phosphorus-deficient (−P) cultures of *Chaetoceros tenuissimus*

Expression values were obtained by reverse transcription–real-time PCR (qRT-PCR; A, C, E, and G) and microarray (B, D, F, and H) assays. The former values mean $2^{-\Delta\Delta C_T}$ compared with C_T values of three reference genes, actin, 18S rRNA, and 28S rRNA; C_T indicates cycle threshold. Error bars of expression values in qRT-PCR assay mean standard deviation (N = 3).

significantly ($P < 0.05$) induced under P-limited conditions. These expression patterns obtained in the qRT-PCR assay well coincided with those in microarray (Fig. 2). Based on the results, this study selected the genes of NRT, GS (04999_orf00005), P_iT, and PhoA as N- and P-stress markers of *C. tenuissimus*.

NRT is a transmembrane protein capable of transporting nitrate to the cell. Many diatom species have several divergent NRTs on the genomes, and their transcriptional expression patterns may be different (Hildebrand & Dahlin 2000, Kang et al. 2007, Song & Ward 2007). Among NRTs, nitrate transporter2 in diatoms appeared to be upregulated in N deficiency (Kang et al. 2007, Song & Ward 2007). We found the NRT gene (37203_orf00003) that was matched to the previously reported those of N-repressible nitrate transporter2 (NRT2), and thus describe the gene as an NRT2 in *C. tenuissimus*. Such transcriptional induction of NRT probably allows the N-stress cells to effectively uptake a small amount of nitrate in the water column and obtain nitrate as soon as it is provided in the water. Concurrently, the obtained NO_3 is reduced to NH_4^+, which is subsequently used for glutamine synthesis. Lower transcriptional induction of NRT2 in cells growing on NO_3 might be associated with the synthesis of intracellular inhibitors, such as NH_4^+ and glutamine (Galván & Fernández 2001).

In bacteria, glutamine synthetase type III (GSIII) would appear to be induced in N-deficient conditions; a gram-negative bacterium *Corynebacterium glutamicum* has a GSIII whose expression is repressed by carbon- and/or nitrogen-replete (Schulz et al. 2001). A cDNA of GSIII was found in *Chaetoceros compressum* (Kinoshita et al. 2009), but its expression pattern is poorly understood at present. The GS gene (04999_orf00005) in *C. tenuissimus* appeared to be induced strongly in a N-deficiency state, which possibly suggests that this diatom, when being in a N-deficient state, is ready to synthesize glutamine immediately after successfully obtaining a N source (e.g., nitrate) in the water column. The GS of *C. tenuissimus* could be a useful marker of the N-deficient state.

The present study found the gene of PhoA in the P-deficient *C. tenuissimus*, which well coincides with our previous study, shows that *C. tenuissimus* cultures induce PhoA activities due to phosphate deficiency (Yamaguchi et al. 2014). Results obtained from the microarray and real-time PCR suggest that *C. tenuissimus*, when being P-stressed, can degrade dissolved organic P (phosphate esters) using PhoA and probably uptake the released P_i immediately via expressed P_iT. Such P utilization may prevent other algae from "snatching" the released P_i.

In gene expression analyses, it is important to select useful internal standards. Several reference genes, such as a heat shock protein (*hsp90*), an elongation factor (*elf*), and 18S rRNA have been studied as internal standards (housekeeping genes) in eukaryotic algae (Siaut et al. 2007, Rosic et al. 2011, Kang et al. 2012). Kang et al. (2012) indicated *elf* as a good reference gene for comparative analyses of *fcp* (fucoxanthin–chlorophyll protein) transcriptions in *C. affinis* and *Skeletonema costatum* among N and P stresses. By using *elf*-like as a reference gene, Shih et al. (2015) examined the mRNA transcriptions in P-stressed *C. affinis* and found Pi-repressible P_iT and PhoA genes, as also shown

in the present study. In our data, however, the expression of an *elf*-like gene is downregulated in the P-stressed cultures of *C. tenuissimu*. By contrast, the expression of actin, 18S rRNA, and 28S RNA in *C. tenuissimus* seems to be tolerably constant. The multiple usage of these reference genes may be important to avoid a misunderstanding of gene expression. We think that P_i-repressible P_iT and PhoA of *C. tenuissimus* would be useful indicators for specific detection of its P state by monitoring mRNA transcriptions with multiple references.

Acknowledgements

This work was supported by JSPS KAKENHI Grant No. JP18H02266 and the Japanese Fisheries Agency-aided project for addressing red tides and oxygen-depleted water masses.

References

Baytut, Ö. et al. (2013) Contributions to the diatom flora of the Black Sea from ultrastructural and molecular studies: New records of *Skeletonema marinoi*, *Pseudo-nitzschia pungens* var. *aveirensis* and *Chaetoceros tenuissimus* for the marine flora of Turkey. *Nova Hedwigia*, **96**, 427-444.

Chen, L. C.-M. et al. (1969). *Bonnemaisonia hamifera* Hariot in nature and in culture. *J. Phycol*., **5**, 211-220.

Galván, A. & Fernández, E. (2001) Eukaryotic nitrate and nitrite transporters. *Cell. Mol. Life Sci.*, **58**, 225-233.

Hildebrand, M. & Dahlin, K. (2000) Nitrate transporter genes from the diatom *Cylindrotheca fusiformis* (Bacillariophyceae): mRNA levels controlled by nitrogen source and by the cell cycle. *J. Phycol*., **36**, 702-713.

Imai, I. et al. (1996) Selenium requirement for growth of a novel red tide flagellate, *Chattonella verruculosa* (Raphidophyceae), in culture. *Fish. Sci.*, **62**, 834-835.

Kang, L.-K. et al. (2007) Influences of nitrogen deficiency on the transcript levels of ammonium transporter, nitrate transporter and glutamine synthetase genes in *Isochrysis galbana* (Isochrysidales, Haptophyta). *Phycologia*, **46**, 521-533.

Kang, L.-K. et al. (2012) Quantification of diatom gene expression in the sea by selecting uniformly transcribed mRNA as the basis for normalization. *Appl. Environ. Microbiol*., **78**, 6051-6058.

Kinoshita, S. et al. (2009) The occurrence of eukaryotic type III glutamine synthetase in the marine diatom *Chaetoceros compressum*. *Mar. Genomics*, **2**, 103-111.

Kooistra, W. H. C. F. et al. (2010) Comparative molecular and morphological phylogenetic analyses of taxa in the *Chaetocerotaceae* (Bacillariophyta). *Phycologia*, **49**, 471-500.

Montresor, M. et al. (2013) Diversity and germination patterns of diatom resting stages at a coastal Mediterranean site. *Mar. Ecol. Prog. Ser*., **484**, 79-95.

Nelson, D. M. et al. (1995) Production and dissolution of biogenic silica in the ocean: Revised global estimates, comparison with regional data and relationship to biogenic sedimentation. *Global Biogeochem. Cycle*, **9**, 359-372.

Rines, J. E. B. & Hargraves, P. E. (1988) The *Chaetoceros* Ehrenberg (Bacillariophyceae) flora of Narragansett Bay, Rhode Island, U.S.A. *Bibl. Phycol.*, **79**, 1-196.

Rosic, N. N. et al. (2011) Validation of housekeeping genes for gene expression studies in *Symbiodinium* exposed to thermal and light stress. *Mar. Biotechnol*., **13**, 355-365.

Schulz, A. A. et al. (2001) Nitrogen and carbon regulation of glutamine synthetase and glutamate synthase in *Corynebacterium glutamicum* ATCC 13032. *FEMS Microbiol. Lett*., **205**, 361-367.

Shih, C.-Y. et al. (2015) Transcriptional responses to phosphorus stress in the marine diatom, *Chaetoceros affinis*, reveal characteristic genes and expression patterns in phosphorus uptake and intracellular recycling. *J. Exp. Mar. Biol. Ecol*., **470**, 43-54.

Siaut, M. et al. (2007) Molecular toolbox for studying diatom biology in *Phaeodactylum tricornutum*. *Gene*, **406**, 23-35.

Song, B. & Ward, B. B. (2007) Molecular cloning and characterization of high-affinity nitrate transporters in marine phytoplankton. *J. Phycol*., **43**, 542-552.

Tomaru, Y. et al. (2011) Dynamics of diatom viruses on the western coast of Japan. *Aquat. Microb. Ecol*., **63**, 223-230.

Tomaru, Y. et al. (2018) Occurrence of the planktonic bloom-forming marine diatom *Chaetoceros tenuissimus* Meunier and its infectious viruses in western Japan. *Hydrobiologia*, **805**, 221-230.

Tomaru, Y. et al. (2014) Temperature alters algicidal activity of DNA and RNA viruses infecting *Chaetoceros tenuissimus*. *Aquat. Microb. Ecol.*, **73**, 171-183.

Toyoda, K. et al. (2010) Application of real-time PCR assay for detection and quantification of bloom-forming diatom *Chaetoceros tenuissimus* Meunier. *Plankton Benthos Res*., **5**, 56-61.

Yamaguchi, H. et al. (2014) Utilization of phosphate diesters by phosphodiesterase-producing marine diatoms. *J. Plankton Res*., **36**, 281-285.

Yamaguchi, H. & Sai, K. (2015) Simulating the vertical dynamics of phosphate and their effects on the growth of harmful algae. *Estuar. Coast. Shelf Sci*., **164**, 425-432.